

Multichromatic quantum superpositions in entangled two-photon absorption spectroscopy

M Wittkop,^a Juan M. Marmolejo-Tejada,^a Martín A. Mosquera^{a,*}

Department of Chemistry and Biochemistry

103 Chemistry and Biochemistry Building, Bozeman, MT-59717, USA

*martinmosquera@montana.edu

March 2, 2023

Abstract

Quantum information science is driving progress in a vast number of scientific and technological areas that cover molecular spectroscopy and matter-light interactions in general. In these fields, the ability to generate quantum mechanically-entangled photons is opening avenues to explore the interaction of molecules with quantum light. This work considers an alternative way of correlating photons by including energy superpositions. We study how the multichromatic quantum superposition, or color superposition of photon-pair states, influences the optical properties of organic chromophores. This work uses electronic structure calculations based on time-dependent density functional theory, and a simple modification of the standard entangled two-photon absorption theory. Our calculations show that it is possible to substantially modify the optical absorption cross section of molecules, where constructive and destructive interferences are computed. The quantum interference effects are more pronounced than the constructive ones. These quantum effects, or related ones, could be observed in quantum spectroscopic experiments where qudit photon states are generated.

1 Introduction

Quantum spectroscopy offers tools to elucidate molecular systems and materials that both expand and complement techniques based on classical light [1, 2, 3]. This has motivated work that is constantly demonstrating the significant transformative potential of quantum light to understand molecular function and open technological opportunities. Such advances are taking place in parallel with scientific and engineering fields such as photonic quantum computing [4, 5], where the precise and accurate control of correlated photons could bring substantial advantages for diverse, cutting-edge applications.

A specific phenomenon that has received widespread attention recently is the absorption and emission of entangled photon pairs by molecules. Entangled two-photon absorption (ETPA) [6], for instance, introduces physical correlations that are not possible in classical two-photon absorption (TPA) spectroscopy [7]. ETPA commonly relies on the generation of entangled photon-pairs, which usually occurs through the well-known spontaneous parametric down conversion (SPDC) process [8]. SPDC provides photon pairs where the polarization of the photons are quantum mechanically correlated, and such entanglement can be verified in EPR-like (Einstein-Podolsky-Rosen) devices [9, 10, 11]. These photons are emitted within an quantum area, and the photons in each entangled pair are delayed with respect to one another [12, 13]. Such delay is expressed in terms of an entanglement time, which endow ETPA techniques with unique properties that to-date continue to be explored by the community. Entangled photons can be emitted through other mechanisms such as molecular pathways [14, 15], quantum dots [16, 17], or semiconducting devices [18, 19].

A family of chromophores have been investigated recently: molecules such as Rhodamine 6G [20], Zinc-TPP [21], and thiophene dendrimers [22], among other dyes [23]. ETPA absorption of a molecular unit is quantified commonly through ETPA cross-sections, which have the same units as classical one-photon cross sections, usually expressed in cm^2 units. Rigorous experimental efforts suggest that ETPA offers considerable quantum advantage over classical TPA (CTPA) [23], especially at low photon (quantum light) fluxes (at extremely low fluxes ETPA will dominate significantly over CTPA). However, the estimation of entangled cross sections with very high accuracy is the subject of current efforts [24, 23]. This is a strong motivation, in our opinion, to further the understanding of the interaction of molecules and

materials with quantum light and their connection to quantum technologies. One can hypothesize that experimental and theoretical techniques will continue to advance in these directions, unlocking unexpected and highly beneficial quantum phenomena in a wide variety of systems.

Experimental and theoretical studies so far have focused on the interplay between single entangled photon pairs and molecules, where the frequencies of the photons are assumed to be given. For example, in degenerate pumping the frequency of both photons are the same. Recently, however, energy superposition of photons has been achieved for individual photons [25, 26, 27] and for photon pairs [18]. Energy superpositions give rise to the well-known “qudit” states, which generalize the concept of the qubit. Also known as color superposition, in this phenomenon, the color of the photons is undetermined, and each single photon is in a superposition of two (or more) colors. Even though the interaction between photon qubit (or qudit) states and molecules has not been reported experimentally so far, their effects can be explored theoretically. We do so in this case for three chromophores of interest: flavin mononucleotide (FMN) [28, 29], topotecan (TPT) [30, 31, 32, 33], and lucifer yellow (LY) [34]. This work studies the molecular absorption of entangled photon-pairs that also feature multichromatic superpositions and polarization entanglement. These photon pairs could form qudits of six-fold dimensionality (or eight-fold if four colors are used); this work, however, focuses on a qubit representation, as specified herein, but a higher-dimensionality of quantum states is possible. We find that the cross sections in this case show signatures of constructive and destructive interferences, depending on the location of the quantum superposition in the Bloch sphere. For a special set of angles in the Bloch sphere, we notice that the destructive interference can be quite substantial, and for other angles, we observed that the absorption cross section can be enhanced by close to an order of magnitude, whereas the quantum interference can lower absorption by up to two orders of magnitude. These findings then suggest the phenomenon of color-superposition could be of interest for additional quantum control of ETPA cross sections and related experiments.

2 Theory

This work focuses on the interaction of photon pairs with vertical electronic excited states only. This is a common approximation that is employed in

CTPA spectroscopy because full vibronic transitions are quite demanding, computationally.

For photon-pairs characterized by two unique frequencies ω_1 and ω_2 , entanglement time T_e , and entanglement area A_e , the absorption cross-section is given by [35]: $\sigma_{f,0} = (4\pi^3\alpha a_0^5)/(A_e\tau_0c) \times g(\omega_T - \Omega_f)|W_{f,0}|^2$, where g is the line shape function, ω_T is the sum of the two photon frequencies, τ_0 is the atomic unit of time ($\tau_0 = m_e a_0^2/\hbar$), Ω_f is the excitation energy for transition from the ground state to the excited state labeled f (the ground state is labeled as the 0-th state), a_0 is the Bohr length, α the fine structure constant, and c the speed of light. The cross-section then has the units that arise from the term $(4\pi^3\alpha a_0^5)/(A_e\tau_0c)$. This result for $\sigma_{f,0}$ can be derived using second perturbation theory and assuming that the photons are modeled as uniform plane wave packets with fronts that are spatially separated by a distance of cT_e . In terms of random photon detection times, the time difference between photon detections is then in average the entanglement time, T_e .

The function $W_{f,0}$ reads:

$$W_{f,0}(\omega_1, \omega_2, T_e) = \sqrt{\frac{\omega_1\omega_2}{T_e}} S_{f,0} \quad (1)$$

where ω_1 and ω_2 are the frequencies of the first and second incoming photons, correspondingly. In the expressed equations, all the frequencies, dipole moments, and entanglement times are expressed in atomic units (a.u.); this includes κ and Γ . The term $S_{f,0}$ represents the transition function (in atomic units):

$$S_{f,0} = \sum_j \frac{(\vec{\mu}_{fj} \cdot \vec{\epsilon}_2)(\vec{\mu}_{j0} \cdot \vec{\epsilon}_1)}{\Omega_j - \omega_1 - i\kappa} \left\{ 1 - \exp[-i(\Omega_j - \omega_1 - i\kappa)T_e] \right\} + (1 \leftrightarrow 2) \quad (2)$$

where κ represents the inverse of the lifetime of the intermediate virtual state, $\vec{\epsilon}_1$ and $\vec{\epsilon}_2$ are the polarizations of the first and second photon, respectively. The transition dipole vector for a transition from ground state to excited state “ j ” is denoted as $\vec{\mu}_{j0}$, whereas $\vec{\mu}_{fj}$ denotes the transition dipole vector for a transition from the j -th excited state into the final state f . The lineshape function g is described in terms of a Lorentzian profile of the form $g(\Delta\omega) = \pi^{-1}(\Gamma/2)/[\Delta\omega^2 + (\Gamma/2)^2]$.

We now consider the two-photon packet as being in a superposition of two states: “MC”, in which the photons are monochromatic ($\omega_1 = \omega_2 = \omega_T/2$), and “BC”, in which the photons are bichromatic, $\omega'_1 \neq \omega'_2$; the “primed”

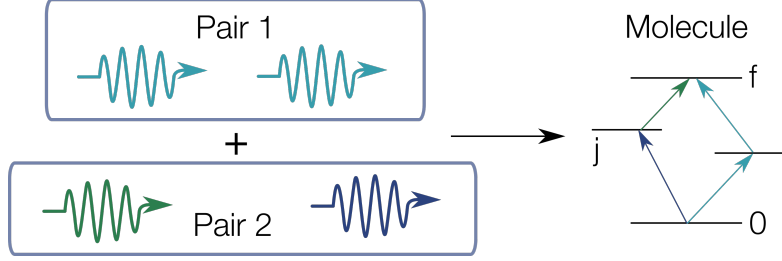


Figure 1: Pictorial representation of the present theoretical model: A two-photon quantum packet is directed towards a molecule. The two-photon state is a quantum superposition of two possible entangled states, a monochromatic pair, labeled “MC”, and a bichromatic pair, referred to as the “BC” pair. The molecule can then be excited through different pathways where different intermediate states are involved in the overall two-photon excitation, as suggested in this figure.

quantities are assigned to the BC state. It is assumed that MC and BC photon-pair quantum states have entanglement times T_e and T'_e , respectively, but have assigned the same area A_e . The quantum superimposed two-photon state is thus described by:

$$|\Psi_\gamma\rangle = \cos\left(\frac{\theta}{2}\right)|MC\rangle + \sin\left(\frac{\theta}{2}\right)e^{i\phi}|BC\rangle \quad (3)$$

we refer to this state as a “multichromatic superposition” (MCS). The MCS is thus controlled by the Bloch sphere parameters θ and ϕ , where $0 \leq \phi \leq 2\pi$ and $0 \leq \theta \leq \pi$. Because the MCS photon configuration obeys the standard linear superposition of states, the function $\tilde{W}_{f,0}$ must also transform as:

$$W_{f,0}^{\text{QS}} = \cos\left(\frac{\theta}{2}\right)W_{f,0}^{\text{MC}} + \sin\left(\frac{\theta}{2}\right)e^{i\phi}W_{f,0}^{\text{BC}} \quad (4)$$

The amplitude $W_{f,0}^{\text{QS}}$, as a quantum mechanical transition element, is also described in terms of the Bloch-sphere angles θ and ϕ . The W functions are evaluated as $W_{f,0}^{\text{MC}} = W_{f,0}(\omega_1, \omega_2, T_e)$ and $W_{f,0}^{\text{BC}} = W_{f,0}(\omega'_1, \omega'_2, T'_e)$. Figure 1 shows a pictorial summary of the theoretical concept explored in this work.

The cross section for a discrete MCS transition of interest is:

$$\sigma_{0 \rightarrow f}^{\text{QS}} = \frac{4\pi^3 \alpha a_0^5}{A_e \tau_0 c} g(0) |W_{f,0}^{\text{QS}}|^2 \quad (5)$$

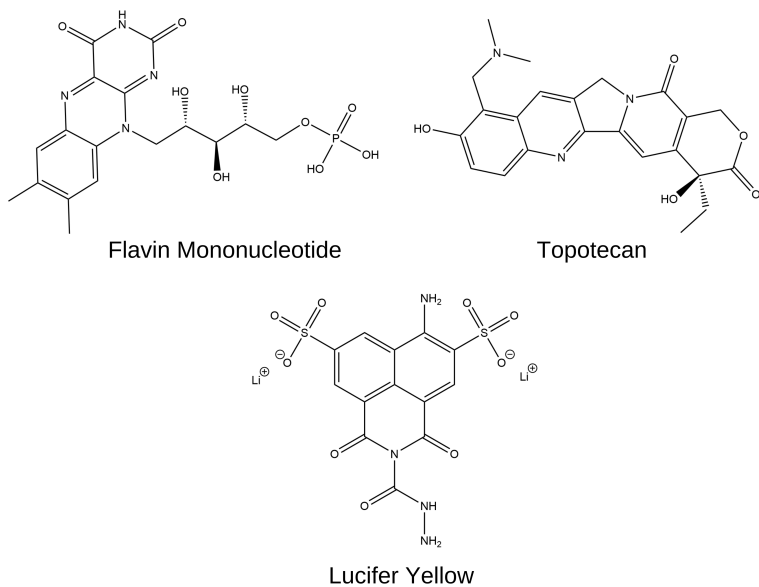


Figure 2: Molecular structures considered in this work: Flavin mononucleotide, topotecan, and lucifer yellow.

where $\omega_{f,0} = \omega_T$, so $g(0) = 2/\pi\Gamma$. The above equation is a relatively simple extension of the standard formula used in standard ETPA spectroscopy, but it now includes the possibility of there being color-superposition. This formula supposes, as expected, that dissipation effects and thereby decoherence in the generation of these MCS photon states are minimal. It is important to notice that perturbation theory demands energy conservation, as the interaction time is assumed to last for a very long time. For this reason we have that $\omega_1 + \omega_2 = \omega'_1 + \omega'_2 = \omega_T$.

3 Computational Method

The transition dipoles are calculated by means of linear-response time-dependent density functional theory (TDDFT). We use the so-called unrelaxed dipoles, or dipoles that come from “CIS-like” linear response TDDFT wavefunctions. This is a practical approximation that works reasonably well, and is computationally efficient. We extract these dipoles with an in-house code that is based on the quantum chemistry suite NWChem [36], version 7.0. We use

the standard B3LYP exchange-correlation functional, and the 6-31G* basis set, which is commonly applied to determine excited-state transitions in the optical regime.

As discussed before, there is yet a source ETPA enhancement that is not well-understood from a theory perspective. In Ref. [37], the use of radiative lifetimes was suggested to obtain ETPA cross-section values in the range of what has been experimentally observable. Motivated by the common practice in TPA theory of using a standard value for the broadening, for the ETPA calculations, we assume a value of Γ that corresponds to 10^{-8} eV, reflecting a final state lifetime of approximately 1.0 ns. For the intermediate state we assume $\kappa = 0.01$ eV. In all the ETPA calculations the entanglement area is $A_e = 1.0 \times 10^{-8}$ cm². For the standard ETPA (non-color superposition), we assume $T_e = 100$ fs. This same value, $T_e = 100$ fs, is applied for the MCS (color superimposed) ETPA, for the BC and MC quantum states of TPT and LY (Figure 2) we take $T_e = T'_e = 100$ fs, but for FMN we set $T_e = 100$ fs and $T'_e = 75$ fs (T'_e being the entanglement time of the BC quantum state).

Classical TPA spectra are computed for comparison as well. For these we take the standard final state broadening factor, the classical equivalent of Γ , as 0.1 eV, and intermediate linewidth, the analogue of κ , as 0.05 eV. We assume that the photons have cross-polarization: so if one photon has horizontal polarization, the other has vertical polarization. The cross sections are averaged with respect to all possible molecular orientations [38].

4 Results and Discussion

To illustrate the proof-of-concept for the effect of color/multichromatic superpositions on the ETPA cross sections, we first compute the conventional TPA spectrum and the standard ETPA spectra. Then, we proceed to examine the MCS-ETPA properties of the chromophores selected for our theoretical study. These chromophores are flavin mononucleotide (FMN), topotecan (TPT), and lucifer yellow (LY); their molecular drawings are shown in Figure 2. FMN is a biomolecule produced from riboflavin that forms part of NADH Hydrogenase, TPT is used as a chemotherapy drug, and LY is utilized in spectroscopic studies. The spectra in this work are reported in terms of half the frequency of the total two-photon frequency. This half-frequency is denoted as $\omega_h = \omega_T/2$.

The theoretical CTPA spectra of FMN, TPT, and LY, are shown in Figure

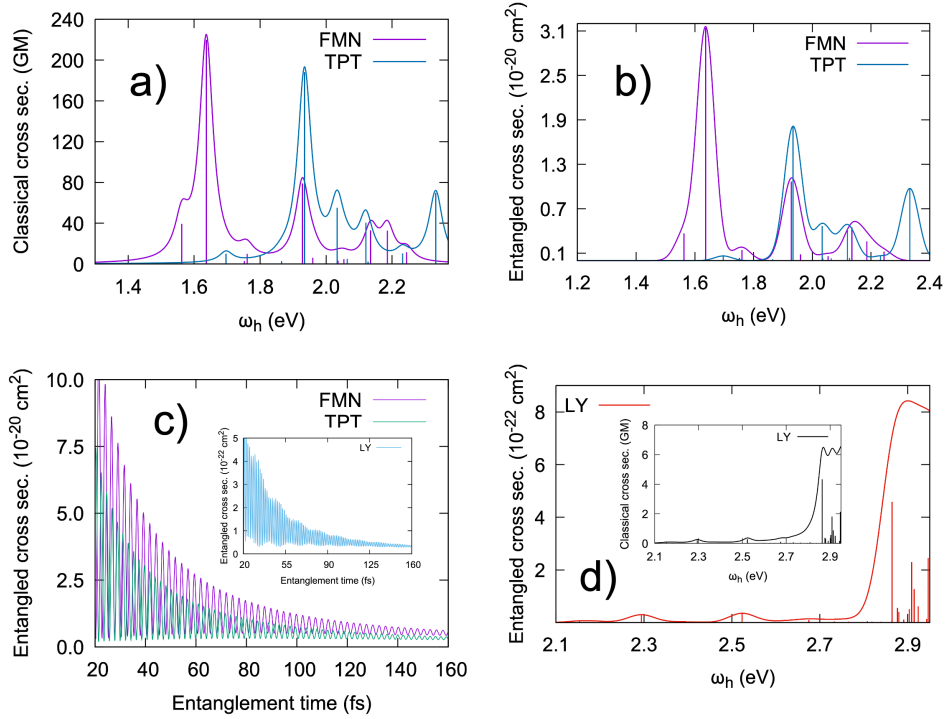


Figure 3: Entangled and classical two-photon absorption cross sections: a) classical TPA profiles of FMN and TPT; b), monochromatic ETPA cross section as a function of ω_h for FMN and TPT; c), ETPA cross section vs. entanglement time for FM, TPT, and LY at energies 1.64, 1.94, and 2.33 eV, respectively. d), ETPA profile of LY, and CTPA cross section (inset).

3.a. and d. (as an inset plot). We note that FMN has a classical TPA cross section of about 220 GM at around a half-frequency of 1.64 eV (760 nm). As is commonly seen in theoretical TPA spectra, the classical TPA shows comparable cross-section values at higher ω_h frequencies. A similar numerical trend is noticed for TPT, where the CTPA cross section is about 188 GM at 1.94 eV (640 nm), and then it slightly decreases to about 41 GM at 2.12 eV, but it raises again to 70 GM around $\omega_h = 2.3$ eV. LY, however, shows a different profile, as can be seen in Figure 3.d, where it is relatively low - under 1 GM for half-frequencies between 2.1 and 2.7 eV, where it raises to about 8 GM at 2.9 eV.

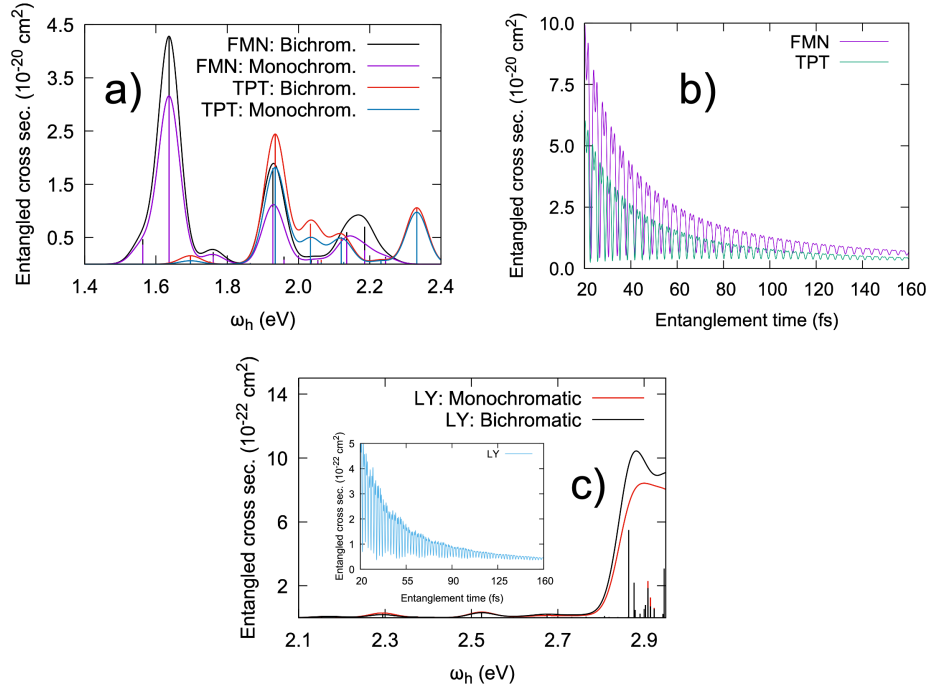


Figure 4: Purely bichromatic ETPA. The frequencies of BC quantum state are $\omega'_1 = 1/3 \times \omega_T$, $\omega'_2 = 2/3 \times \omega_T$: a), BC ETPA spectra of FMN and TPT, and their comparison to the monochromatic counterpart; b), variation of FMN and TPT BC ETPA cross section as a function of the entanglement time, the frequencies ω_h are the same as in Figure 3.c; c), BC ETPA spectrum of LY, inset shows dependency on T_e at 2.9 eV.

Regarding standard monochromatic ETPA ($\omega_1 = \omega_2 = \omega_h$), Figure 3.b

shows the entangled cross section profiles of FMN and TPT, and Figure 3.d shows that of LY. For these three systems we use $T_e = 100$ fs. For these systems we see a correlation between the CTPA and ETPA spectra, however, for TPT such connection between classical and entangled TPA is somewhat less evident, as there are some changes between relative peak heights. FMN and TPT have ETPA cross section values in the same order of magnitude, 10^{-20} cm². The maximum values of FMN and TPT occur at the same frequencies as their classical TPA counterparts, with values close to 3.0×10^{-20} cm² and 1.8×10^{-20} cm², respectively. As mentioned earlier, for the three systems considered we use the same linewidth factors. The entanglement time is another variable that affects the magnitude of the ETPA cross sections; the effect of varying this is displayed in Figure 3.c, where we observe, as expected, that the cross section can vary by one order of magnitude, or more, if the T_e is further increased beyond the plot time range. For the LY chromophore, we observe theoretical cross section values lower than those of FMN and TPT, which indicate ETPA activity around 2.3 eV (540 nm) and 2.5 eV (496 nm), and then higher values at 2.9 eV (430 nm).

Figure 4 displays the standard ETPA spectra under a non-degenerate condition, where the two photons have different frequencies. In this case we choose $\omega'_1 = \omega_T/3$, and $\omega'_2 = 2\omega_T/3$ and refer to this as “bichromatic ETPA”. The bichromatic ETPA spectrum of each molecule shows a few differences with respect to the monochromatic ones. These are mainly a slight enhancement of the ETPA cross section, up to 30 %. However, between 2.0 and 2.4 eV, the degenerate-pumping ETPA spectrum of TPT is not improved much by the bichromatic condition. As in the degenerate case, the cross section at low photon frequency varies by about one order of magnitude for T_e in the range 20 - 100 fs. Due to the parameter κ , the ETPA cross-sections in all cases have their oscillations damped. The oscillatory pattern of the BC ETPA case is slightly different than in the monochromatic case, but not too significantly.

Having determined the difference between the separate MC and BC ETPA cases, we now proceed to examine the multichromatic quantum superposition effect, as expressed in Equation (4). We focus on highest intensity transitions, which happen at 1.64, 1.94, and 2.9 eV for FMN, TPT, and LY, respectively. Figure 5.a shows the comparison between the quantum superposition effect and the standard MC and BC ETPA cases where there is no superposition. For a polar angle of $\theta = 60^\circ$, the two-photon state is a quantum mixture of 75 % the monochromatic state, and 25 % the bichromatic state, yet we

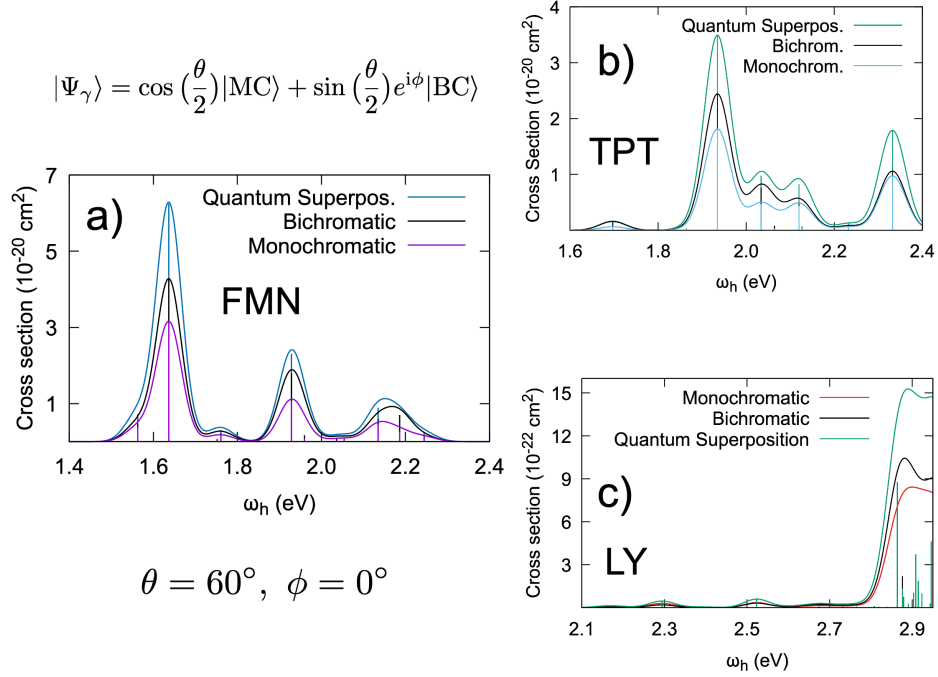


Figure 5: ETPA cross sections based on quantum color superpositions, or quantum MCS. The Bloch sphere parameters are fixed and taken as $\theta = 60^\circ$ and $\phi = 0^\circ$. For TPT and LY the entanglement times of the BC and MC states are the same $T_e = T'_e = 100$ fs, but for FMN we study $T_e = 100$ fs and $T'_e = 75$ fs. a) Shows the standard quantum MCS ETPA spectra of FMN, b), that of TPT, and c), LY.

see that the quantum cross section is over 100 % enhanced with respect to the monochromatic ETPA case, for a frequency of 1.64 eV. A similar enhancement takes place for TPT and LY (Figures 5.b and .c, respectively), at 1.94 eV and 2.9 eV, correspondingly. This enhancement is also due to setting the phase factor as $\phi = 0^\circ$. In additional preliminary calculations, we have noted $\phi = 0^\circ$ leads to quantum *constructive* effects.

For the three molecular systems, FMN, TPT, and LY, Figure 6 shows the variation of cross-section values with respect to the Bloch sphere parameters (again, we examine this at the frequencies 1.64 eV, 1.94 eV, and 2.9 eV, correspondingly). The most interesting behavior in terms of quantum constructive effects takes place at the points where theta is between 60° and 120° , while ϕ being close to 0° or 180° . There is thus a region of constructive interference, where the enhancement in cross section doubles. A higher enhancement is possible for different combinations of entanglement times [39], or if the quantum superposition has an additional constructive effect that improves the lifetimes of the intermediate and final excited states involved in the ETPA quantum process (which are not explored in this work). On the other hand, a significant *destructive* quantum interference takes place in a region center around $\theta = 90^\circ$ and $\phi = 180^\circ$. The cross section value drops by up to two orders of magnitude under the current parameter selection. It drops by two orders of magnitude (from 10^{-20} cm² to 10^{-22} cm²) for FMN, one order of magnitude for TPT, and two for LY. Figure 6.b shows the dependency of σ with respect to θ for $\phi = 90^\circ$. Clearly, the quantum superposition engenders behaviors that are not possible under the separate circumstances, which is to be expected from this type of phenomenon. Therefore, besides present in coherent electronic transfer [40], destructive quantum interference is also possible in photon absorption.

As is common in quantum coherent phenomena, there are conditions that must be satisfied to observe quantum superposition effects. One of them is the suppression of decoherence related to vibrational degrees of freedom. These occur during the emission of entangled photons and the absorption of these. It is currently a subject of intensive research determining the influence of entangled photons on the lifetime of excited states. But there are indications that such lifetimes are enhanced by entangled photon absorption [41]. In this work, we assumed fixed linewidth parameters in line with values used before [37] to obtain theoretical values consistent with experimental measurements. However, as in standard ETPA, the effect of MCS on the lifetimes could be a subject of further research as well, as additional quantum correlations could

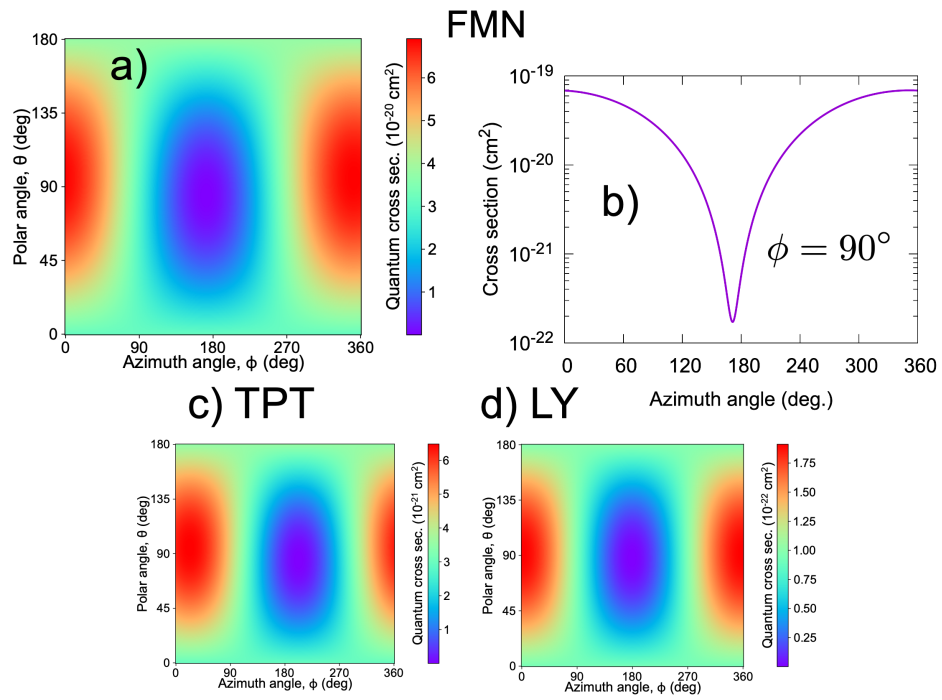


Figure 6: Two-dimensional heat plots for FMN (subfigure a) at $\omega_h = 1.64$ eV, TPT (subfigure c) at 1.94 eV, and LY (subfigure d) at 2.9 eV, and a “cut” for $\phi = 90^\circ$ for the FMN system.

have unexpected consequences on electronic lifetimes and other quantum properties.

5 Conclusion

In this work we investigated the interaction between entangled photon pairs, that in addition to having the standard polarization correlation, feature energy superpositions. That is, the frequency of the photons are undetermined prior to interaction with matter. We referred to this phenomenon as a multichromatic superposition. The state of the entangled photon pair was represented in the well-known Bloch sphere, or qubit space. In comparison to standard ETPA simulations, we observed the emergence of constructive and destructive effects in the quantum cross section profiles. The enhancement (or constructive) of cross section was computed to be improved by nearly a 100 %, whereas the destructive interference could reduce the cross section by around two orders of magnitude. Our work then suggests that these types of coherent effects could be added to the toolkits of quantum control within the context of optical quantum spectroscopy.

6 Acknowledgments

The authors kindly thank the MonArk NSF Quantum Foundry supported by the National Science Foundation Q-AMASE-i program under NSF award No. DMR-1906383.

References

- [1] Audrey Eshun, Oleg Varnavski, Juan P Villabona-Monsalve, Ryan K Burdick, and Theodore Goodson III. Entangled photon spectroscopy. *Accounts Chem. Res.*, 55(7):991–1003, 2022.
- [2] Ying-Zhong Ma and Benjamin Doughty. Nonlinear optical microscopy with ultralow quantum light. *J. Phys. Chem. A*, 125(40):8765–8776, 2021.

- [3] Bahaa EA Saleh, Bradley M Jost, Hong-Bing Fei, and Malvin C Teich. Entangled-photon virtual-state spectroscopy. *Phys. Rev. Lett.*, 80(16):3483, 1998.
- [4] Emanuele Pelucchi, Giorgos Fagas, Igor Aharonovich, Dirk Englund, Eden Figueroa, Qihuang Gong, Hübel Hannes, Jin Liu, Chao-Yang Lu, Nobuyuki Matsuda, et al. The potential and global outlook of integrated photonics for quantum technologies. *Nature Reviews Physics*, 4(3):194–208, 2022.
- [5] Sergei Slussarenko and Geoff J Pryde. Photonic quantum information processing: A concise review. *Appl. Phys. Rev.*, 6(4):041303, 2019.
- [6] Frank Schlawin, Konstantin E Dorfman, and Shaul Mukamel. Entangled two-photon absorption spectroscopy. *Accounts Chem. Res.*, 51(9):2207–2214, 2018.
- [7] Oleg Varnavski and Theodore Goodson III. Two-photon fluorescence microscopy at extremely low excitation intensity: The power of quantum correlations. *J. Am. Chem. Soc.*, 142(30):12966–12975, 2020.
- [8] Chao Zhang, Yun-Feng Huang, Bi-Heng Liu, Chuan-Feng Li, and Guang-Can Guo. Spontaneous parametric down-conversion sources for multiphoton experiments. *Advanced Quantum Technologies*, 4(5):2000132, 2021.
- [9] DN Klyshko. Combine epr and two-slit experiments: Interference of advanced waves. *Phys. Lett. A*, 132(6-7):299–304, 1988.
- [10] DN Klyshko. A simple method of preparing pure states of an optical field, of implementing the einstein–podolsky–rosen experiment, and of demonstrating the complementarity principle. *Soviet Physics Uspekhi*, 31(1):74, 1988.
- [11] Áulide Martínez-Tapia, Samuel Corona-Aquino, Chenglong You, Rui-Bo Jin, Omar S Magaña-Loaiza, Shi-Hai Dong, Alfred B U’Ren, and Roberto de J León-Montiel. Witnessing entangled two-photon absorption via quantum interferometry. *arXiv preprint arXiv:2208.11387*, 2022.

- [12] YH Shih and AV Sergienko. A two-photon interference experiment using type ii optical parametric down conversion. *Phys. Lett. A*, 191(3-4):201–207, 1994.
- [13] AV Sergienko, YH Shih, and MH Rubin. Experimental evaluation of a two-photon wave packet in type-ii parametric downconversion. *JOSA B*, 12(5):859–862, 1995.
- [14] Mohammad Rezai, Jörg Wrachtrup, and Ilja Gerhardt. Polarization-entangled photon pairs from a single molecule. *Optica*, 6(1):34–40, 2019.
- [15] Pietro Lombardi, Maja Colautti, Rocco Duquennoy, Ghulam Murtaza, Prosenjit Majumder, and Costanza Toninelli. Triggered emission of indistinguishable photons from an organic dye molecule. *Appl. Phys. Lett.*, 118(20):204002, 2021.
- [16] Francesco Basso Basset, Francesco Salusti, Lucas Schweickert, Michele B Rota, Davide Tedeschi, Saimon F Covre da Silva, Emanuele Roccia, Val Zwiller, Klaus D Jöns, Armando Rastelli, et al. Quantum teleportation with imperfect quantum dots. *npj Quantum Inf.*, 7(1):7, 2021.
- [17] Daniel Huber, Marcus Reindl, Johannes Aberl, Armando Rastelli, and Rinaldo Trotta. Semiconductor quantum dots as an ideal source of polarization-entangled photon pairs on-demand: a review. *J. Optics*, 20(7):073002, 2018.
- [18] Michael Kues, Christian Reimer, Piotr Roztocky, Luis Romero Cortés, Stefania Sciara, Benjamin Wetzler, Yanbing Zhang, Alfonso Cino, Sai T Chu, Brent E Little, et al. On-chip generation of high-dimensional entangled quantum states and their coherent control. *Nature*, 546(7660):622–626, 2017.
- [19] Davide Grassani, Stefano Azzini, Marco Liscidini, Matteo Galli, Michael J Strain, Marc Sorel, JE Sipe, and Daniele Bajoni. Micrometer-scale integrated silicon source of time-energy entangled photons. *Optica*, 2(2):88–94, 2015.
- [20] Dmitry Tabakaev, Matteo Montagnese, Geraldine Haack, Luigi Bonacina, J-P Wolf, Hugo Zbinden, and RT Thew. Energy-time-entangled two-photon molecular absorption. *Phys. Rev. A*, 103(3):033701, 2021.

- [21] Ryan K Burdick, George C Schatz, and Theodore Goodson III. Enhancing entangled two-photon absorption for picosecond quantum spectroscopy. *J. Am. Chem. Soc.*, 143(41):16930–16934, 2021.
- [22] M R Harpham, Ö Süzler, Chang-Qi Ma, Peter Bäuerle, and Theodore Goodson III. Thiophene dendrimers as entangled photon sensor materials. *J. Am. Chem. Soc.*, 131(3):973–979, 2009.
- [23] Kristen M Parzuchowski, Alexander Mikhaylov, Michael D Mazurek, Ryan N Wilson, Daniel J Lum, Thomas Gerrits, Charles H Camp Jr, Martin J Stevens, and Ralph Jimenez. Setting bounds on entangled two-photon absorption cross sections in common fluorophores. *Phys. Rev. Appl.*, 15(4):044012, 2021.
- [24] Alexander Mikhaylov, Ryan N Wilson, Kristen M Parzuchowski, Michael D Mazurek, Charles H Camp Jr, Martin J Stevens, and Ralph Jimenez. Hot-band absorption can mimic entangled two-photon absorption. *J. Phys. Chem. Lett.*, 13(6):1489–1493, 2022.
- [25] Eva Zakka-Bajjani, François Nguyen, Minhya Lee, Leila R Vale, Raymond W Simmonds, and José Aumentado. Quantum superposition of a single microwave photon in two different ‘colour’ states. *Nat. Phys.*, 7(8):599–603, 2011.
- [26] Philipp Treutlein. Photon qubit is made of two colors. *Physics*, 9:135, 2016.
- [27] Stéphane Clemmen, Alessandro Farsi, Sven Ramelow, and Alexander L Gaeta. Ramsey interference with single photons. *Phys. Rev. Lett.*, 117(22):223601, 2016.
- [28] Juan P Villabona-Monsalve, Oleg Varnavski, Bruce A Palfey, and Theodore Goodson III. Two-photon excitation of flavins and flavoproteins with classical and quantum light. *J. Am. Chem. Soc.*, 140(44):14562–14566, 2018.
- [29] Rachael J Homans, Raja U Khan, Michael B Andrews, Annemette E Kjeldsen, Louise S Natrajan, Steven Marsden, Edward A McKenzie, John M Christie, and Alex R Jones. Two photon spectroscopy and microscopy of the fluorescent flavoprotein, ilov. *Phys. Chem. Chem. Phys.*, 20(25):16949–16955, 2018.

- [30] Thomas G Burke, Henryk Malak, Ignacy Gryczynski, Zihou Mi, and Joseph R Lakowicz. Fluorescence detection of the anticancer drug topotecan in plasma and whole blood by two-photon excitation. *Anal. Biochem.*, 242(2):266–270, 1996.
- [31] Peter TC So, Chen Y Dong, Barry R Masters, and Keith M Berland. Two-photon excitation fluorescence microscopy. *Ann. Rev. Biomed. Eng.*, 2(1):399–429, 2000.
- [32] Asma Yasmeeen Khan and Gopinatha Suresh Kumar. Exploring the binding interaction of potent anticancer drug topotecan with human serum albumin: Spectroscopic, calorimetric and fibrillation study. *J. Biomol. Struct. Dyn.*, 36(9):2463–2473, 2018.
- [33] Maria Rosaria di Nunzio, YiLun Wang, and Abderrazzak Douhal. Spectroscopy and dynamics of topotecan anti-cancer drug comprised within cyclodextrins. *J Photoch. Photobio. A*, 266:12–21, 2013.
- [34] Arne S Kristoffersen, Svein R Erga, Børge Hamre, and Øyvind Frette. Testing fluorescence lifetime standards using two-photon excitation and time-domain instrumentation: rhodamine b, coumarin 6 and lucifer yellow. *J. Fluoresc.*, 24:1015–1024, 2014.
- [35] Hong-Bing Fei, Bradley M Jost, Sandu Popescu, Bahaa EA Saleh, and Malvin C Teich. Entanglement-induced two-photon transparency. *Phys. Rev. Lett.*, 78(9):1679, 1997.
- [36] Marat Valiev, Eric J Bylaska, Niranjana Govind, Karol Kowalski, Tjerk P Straatsma, Hubertus JJ Van Dam, Dunyou Wang, Jarek Nieplocha, Edoardo Apra, Theresa L Windus, and W A de Jong. Nwchem: A comprehensive and scalable open-source solution for large scale molecular simulations. *Comput. Phys. Commun.*, 181(9):1477–1489, 2010.
- [37] Gyeongwon Kang, Kobra Nasiri Avanaki, Martín A Mosquera, Ryan K Burdick, Juan P Villabona-Monsalve, Theodore Goodson III, and George C Schatz. Efficient modeling of organic chromophores for entangled two-photon absorption. *J. Am. Chem. Soc.*, 142(23):10446–10458, 2020.

- [38] PR Monson and WM McClain. Polarization dependence of the two-photon absorption of tumbling molecules with application to liquid 1-chloronaphthalene and benzene. *J. Chem. Phys.*, 53(1):29–37, 1970.
- [39] Sajal Kumar Giri and George C Schatz. Manipulating two-photon absorption of molecules through efficient optimization of entangled light. *J. Phys. Chem. Lett.*, 13(43):10140–10146, 2022.
- [40] Justin P Bergfield, Henry M Heitzer, Colin Van Dyck, Tobin J Marks, and Mark A Ratner. Harnessing quantum interference in molecular dielectric materials. *ACS Nano*, 9(6):6412–6418, 2015.
- [41] Federica Ricci, Haraprasad Mandal, Muaaz Wajahath, Ryan K Burdick, Juan P Villabona-Monsalve, Saber Hussain, and Theodore Goodson III. Investigations of coherence in perovskite quantum dots with classical and quantum light. *J. Phys. Chem. C*, 2023.